**Electronic Supplementary Information for**

# Oxidation of Magnetite Nanoparticles: Impact on Surface and Crystal Properties

S. P. Schwaminger,[a] D. Bauer,[a] P. Fraga-García,[a] F. E. Wagner,[b] S. Berensmeier*[a]

[a]Bioseparation Engineering Group, Technical University of Munich, Boltzmannstraße 15, Garching, 85748, Germany

[b]Physik-Department E15, Technical University of Munich, James-Franck-Straße 1, Garching, 85748, Germany

*Author to whom correspondence should be addressed

Email: s.berensmeier@tum.de

**Table S1:** Size of synthesised and oxidised samples as calculated with the Scherrer equation from XRD data; lattice constant calculated from the Bragg equation.

| Sample | Size, nm | Lattice constant, Å |
|---|---|---|
| Magnetite | 7.2 | 8.399 |
| Air-15 min | 7.3 | 8.369 |
| Air-2 h | 8.5 | 8.365 |
| Air-7 h | 7.9 | 8.360 |
| Air-24 h | 7.3 | 8.363 |
| HNO3-15min | 8.4 | 8.362 |
| HNO3-2 h | 6.8 | 8.362 |
| HNO3-24 h | 8.0 | 8.349 |

Scherrer equation for spherically-shaped particles measured with Mo Kα radiation:

$$L = \frac{0.89 \cdot 0.07093\ nm}{\Delta 2\theta \cdot cos(\theta)}$$

Bragg equation for cubic system:

$$a = \sqrt{\frac{(0.7093\ \text{Å})^2}{4 \cdot \sin^2\theta}(h^2 + k^2 + l^2)}$$

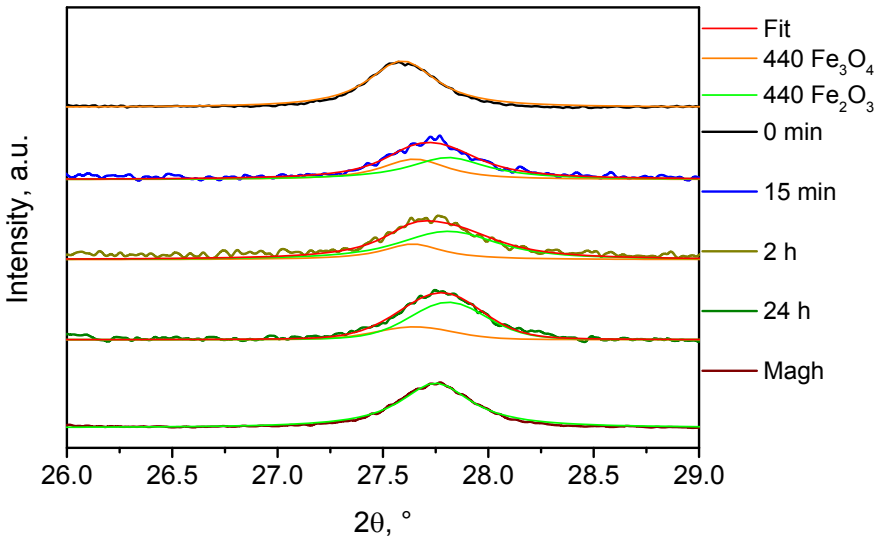


**Figure S2:** Deconvolution of the 440 reflex of freeze-dried aliquots of the harsh oxidation experiment measured with X-ray diffraction using Mo Kα radiation.

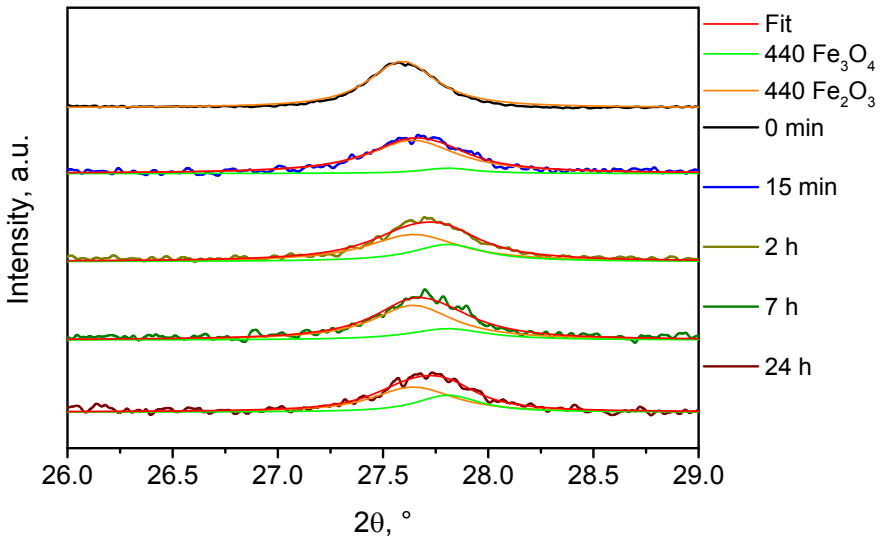


**Figure S3:** Deconvolution of the 440 reflex of freeze-dried aliquots of the mild oxidation experiment measured with X-ray diffraction using Mo Kα radiation.

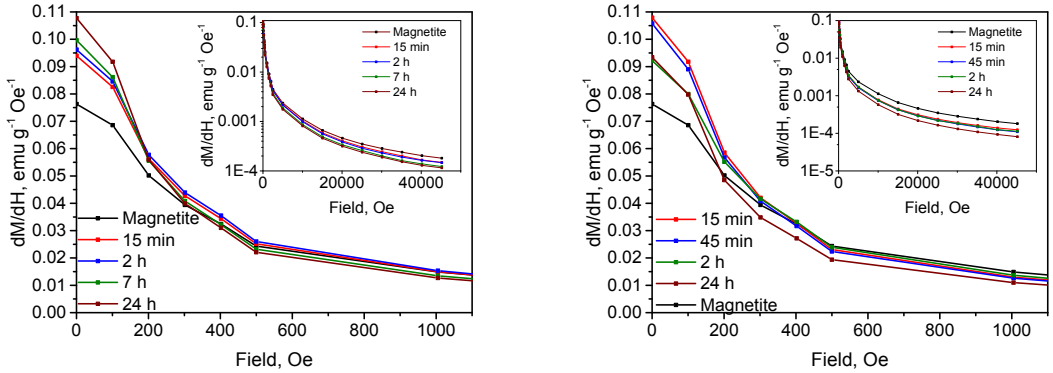


**Figure S4:** Differential susceptibility curves of particles oxidised under mild (left) and harsh (right) oxidation conditions.

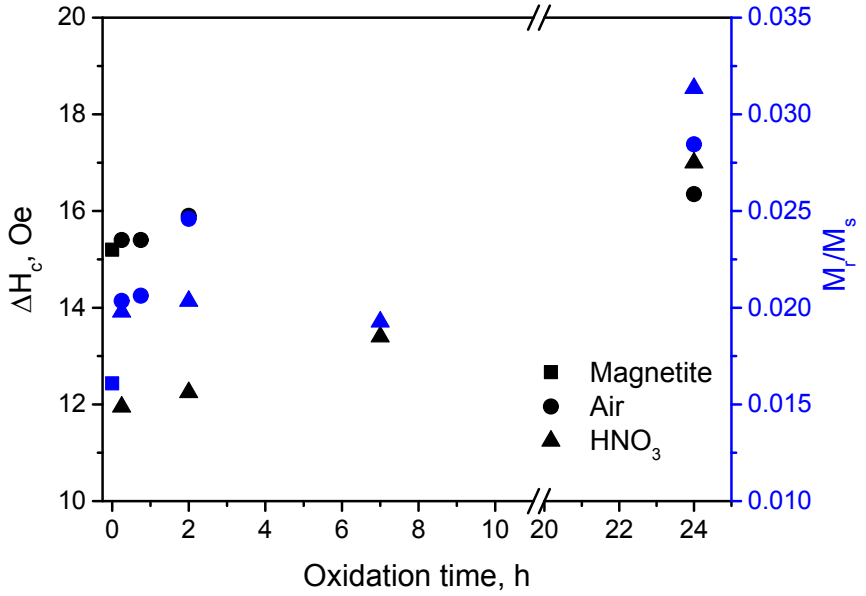


**Figure S5:** Coercivity and reduced remanence measured with a SQUID magnetometer of the synthesised magnetite and the oxidised nanoparticles as a function of the oxidation time.

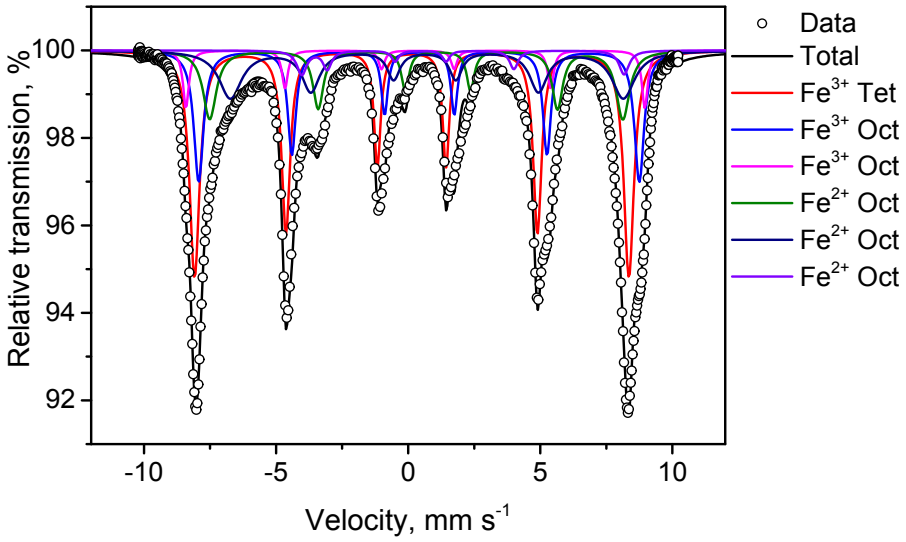


**Figure S6:** Mössbauer spectrum of as-synthesised magnetite nanoparticles frozen in an alkaline NaOH solution at 4.2 K. The spectrum is fitted with a tetrahedral $Fe^{3+}$ component that diverges from octahedral $Fe^{3+}$ by isomeric shift. Three $Fe^{2+}$ components were used with a significantly smaller hyperfine field than the ferric components.

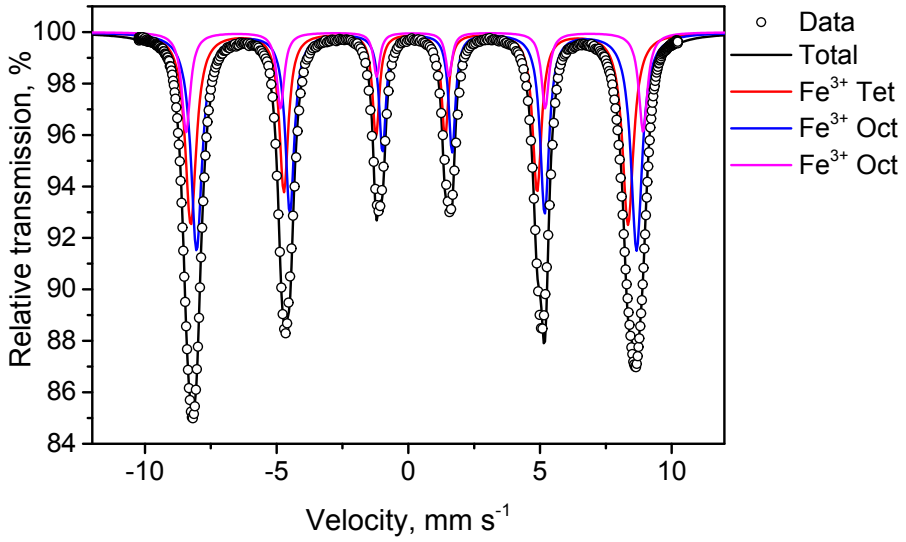


**Figure S7:** Mössbauer spectrum, measured at 4.2 K, of synthesised maghemite nanoparticles. The spectrum is fitted with a tetrahedral $Fe^{3+}$ component that diverges from octahedral $Fe^{3+}$ by isomeric shift.

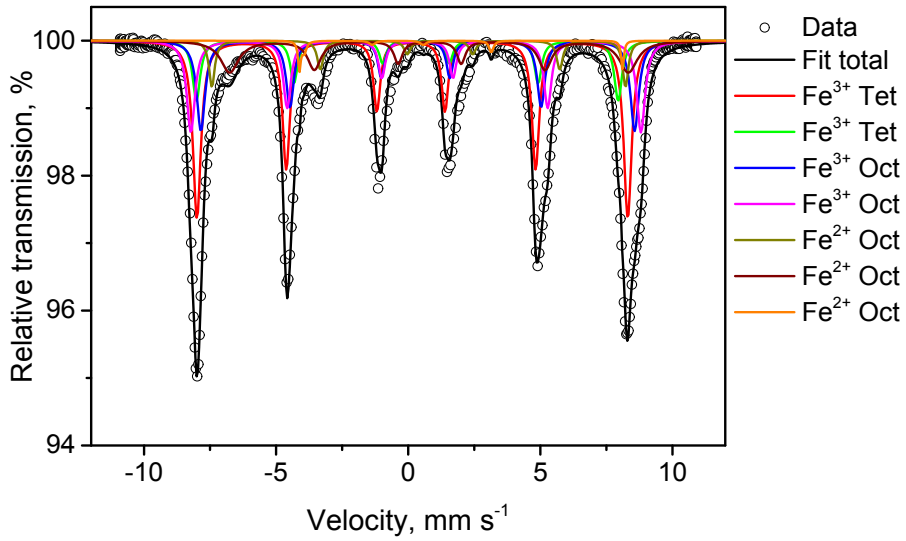


**Figure S8:** Mössbauer spectrum, measured at 4.2 K, of as-synthesised magnetite nanoparticles. The spectrum is fitted with a tetrahedral $Fe^{3+}$ component that diverges from octahedral $Fe^{3+}$ by isomeric shift. Three $Fe^{2+}$ components were used with a significantly smaller hyperfine field than the ferric components.

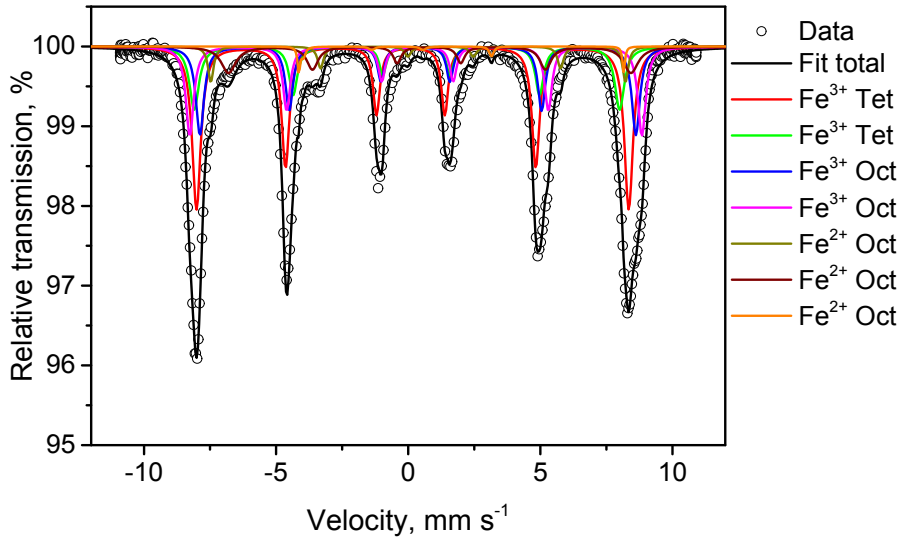


**Figure S9:** Mössbauer spectrum, measured at 4.2 K, of synthesised magnetite nanoparticles oxidised for 15 minutes at 60°C under ambient atmosphere. The spectrum is fitted with a tetrahedral $Fe^{3+}$ component that diverges from octahedral $Fe^{3+}$ by isomeric shift. Three $Fe^{2+}$ components were used with a significantly smaller hyperfine field than the ferric components.

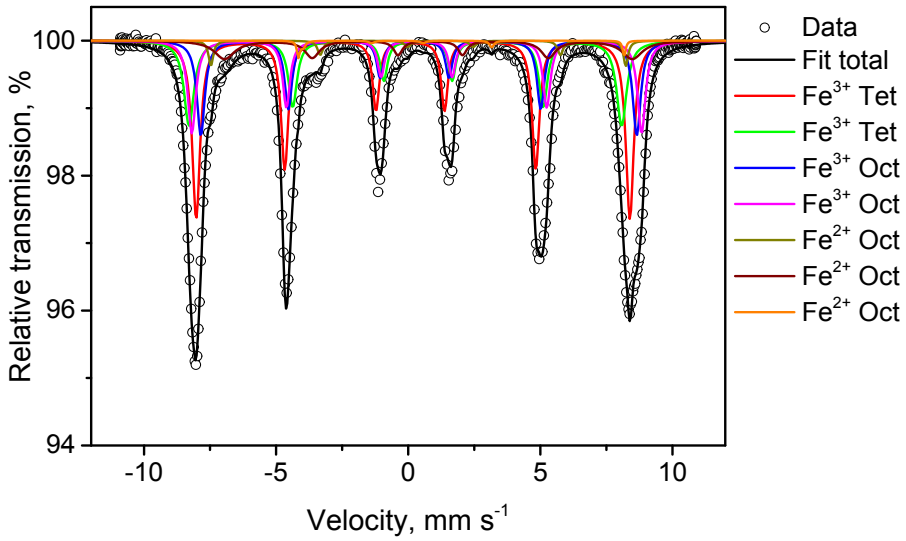


**Figure S10:** Mössbauer spectrum, measured at 4.2 K, of synthesised magnetite nanoparticles oxidised for 2 hours at 60°C under ambient atmosphere. The spectrum is fitted with a tetrahedral $Fe^{3+}$ component that diverges from octahedral $Fe^{3+}$ by isomeric shift. Three $Fe^{2+}$ components were used with a significantly smaller hyperfine field than the ferric components.

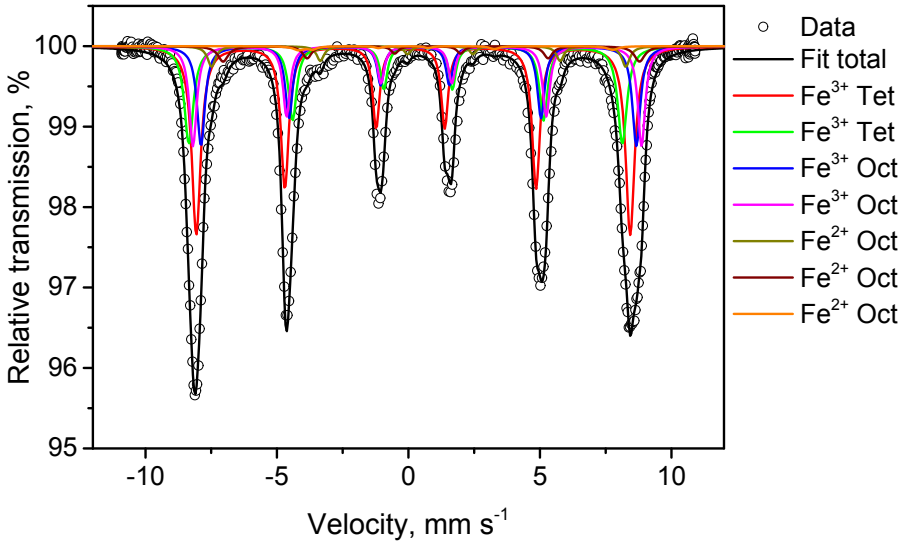


**Figure S11:** Mössbauer spectrum, measured at 4.2 K, of synthesised magnetite nanoparticles oxidised for 7 hours at 60°C under ambient atmosphere. The spectrum is fitted with a tetrahedral $Fe^{3+}$ component that diverges from octahedral $Fe^{3+}$ by isomeric shift. Three $Fe^{2+}$ components were used with a significantly smaller hyperfine field than the ferric components.

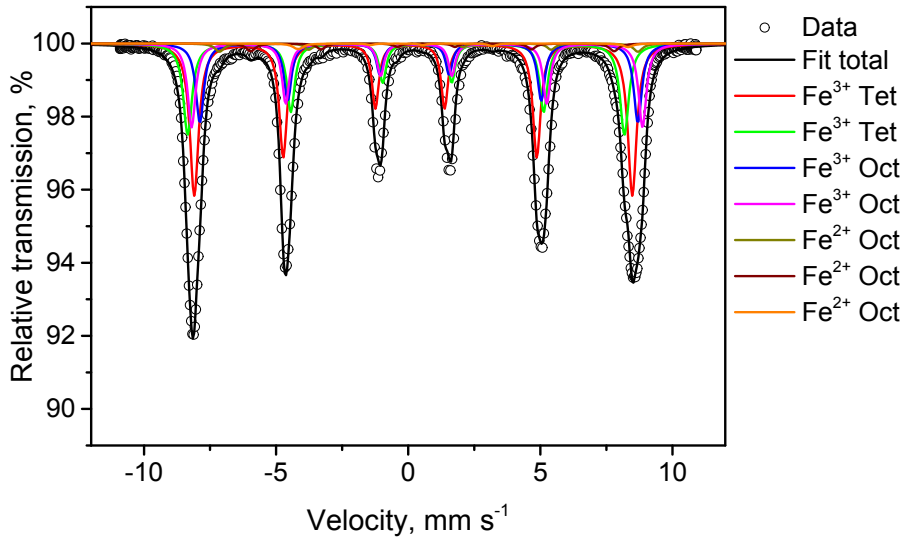


**Figure S12:** Mössbauer spectrum, measured at 4.2 K, of synthesised magnetite nanoparticles oxidised for 24 hours at 60°C under ambient atmosphere. The spectrum is fitted with a tetrahedral $Fe^{3+}$ component that diverges from octahedral $Fe^{3+}$ by isomeric shift. Three $Fe^{2+}$ components were used with a significantly smaller hyperfine field than the ferric components.

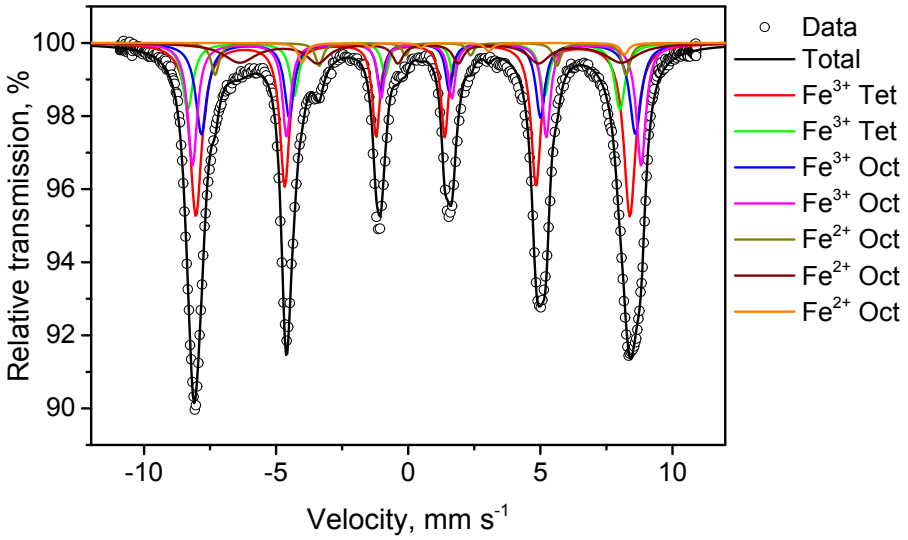


**Figure S13:** Mössbauer spectrum, measured at 4.2 K, of synthesised magnetite nanoparticles oxidised for 15 minutes at 60°C in 1 M $HNO_3$ under ambient atmosphere. The spectrum is fitted with a tetrahedral $Fe^{3+}$ component that diverges from octahedral $Fe^{3+}$ by isomeric shift. Three $Fe^{2+}$ components were used with a significantly smaller hyperfine field than the ferric components.

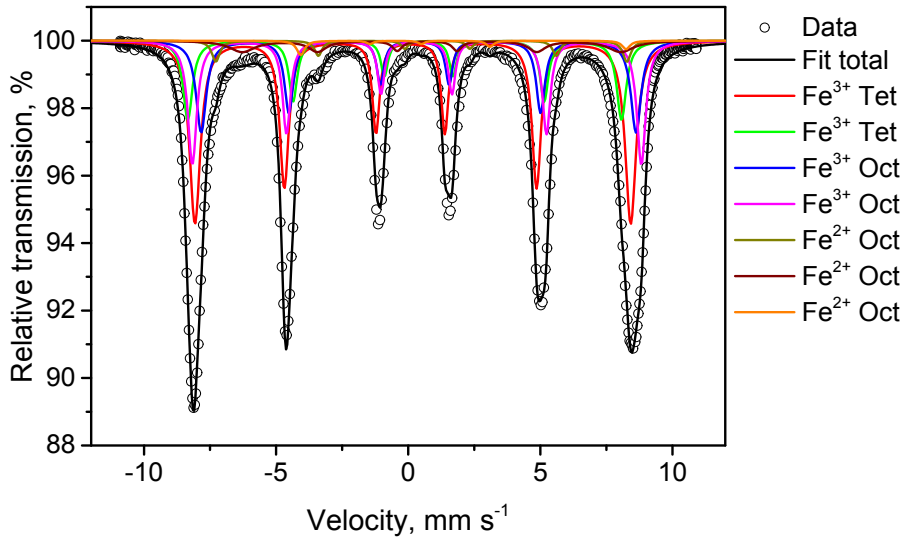


**Figure S14:** Mössbauer spectrum, measured at 4.2 K, of synthesised magnetite nanoparticles oxidised for 45 minutes at 60°C in 1 M $HNO_3$ under ambient atmosphere. The spectrum is fitted with a tetrahedral $Fe^{3+}$ component that diverges from octahedral $Fe^{3+}$ by isomeric shift. Three $Fe^{2+}$ components were used with a significantly smaller hyperfine field than the ferric components.

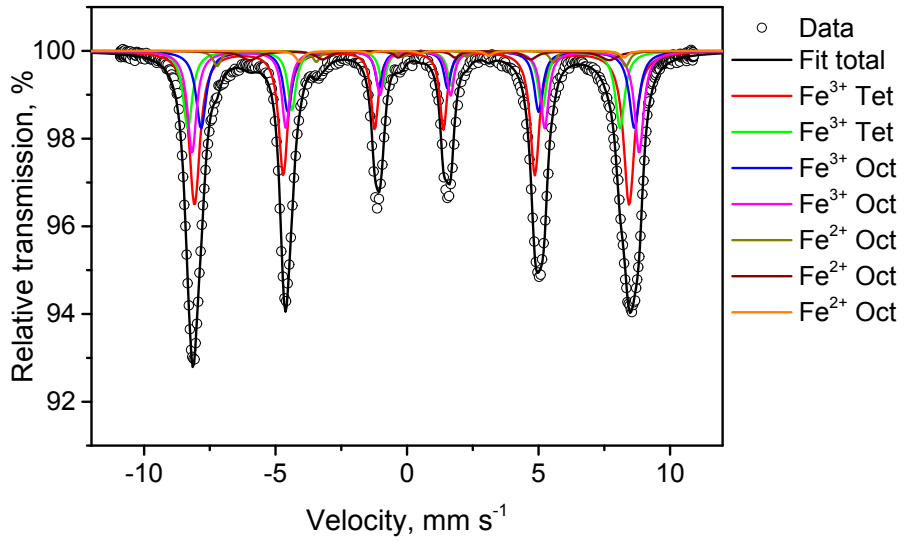


**Figure S15:** Mössbauer spectrum, measured at 4.2 K, of synthesised magnetite nanoparticles oxidised for 2 hours at 60°C in 1 M $HNO_3$ under ambient atmosphere. The spectrum is fitted with a tetrahedral $Fe^{3+}$ component that diverges from octahedral $Fe^{3+}$ by isomeric shift. Three $Fe^{2+}$ components were used with a significantly smaller hyperfine field than the ferric components.

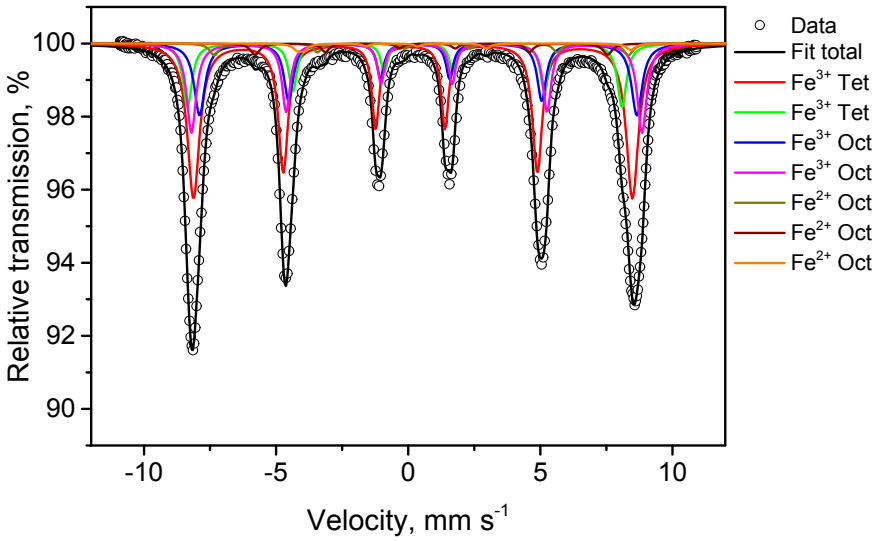


**Figure S16:** Mössbauer spectrum, measured at 4.2 K, of synthesised magnetite nanoparticles oxidised for 24 hours at 60°C in 1 M $HNO_3$ under ambient atmosphere. The spectrum is fitted with a tetrahedral $Fe^{3+}$ component that diverges from octahedral $Fe^{3+}$ by isomeric shift. Three $Fe^{2+}$ components were used with a significantly smaller hyperfine field than the ferric components.

**Table S17:** The iron ion components were fitted according to their isomer shift and magnetic hyperfine field. Iron ions on the tetrahedral vacancies were fitted with the lowest isomer shift, while the trivalent iron ions on octahedral vacancies were fitted with the largest field. The divalent components were fitted with the smallest field and the largest isomer shift.

| | Isomer shift (mm $s^{-1}$) | Hyperfine field (T) |
|---|---|---|
| Tet $Fe^{3+}$ | 0.13 | 50.6-51.5 |
| Oct $Fe^{3+}$ | 0.32-0.42 | 50.9-53.9 |
| $Fe^{2+}$ | 0.7-1.3 | 37.0-49.1 |

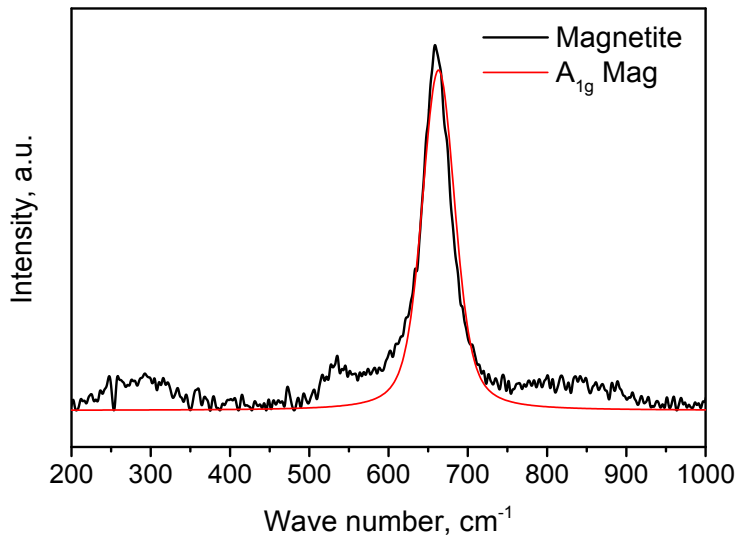

**Figure S18:** Raman spectrum of magnetite suspended in NaOH directly after the synthesis recorded with 488 nm at 0.4 mW.

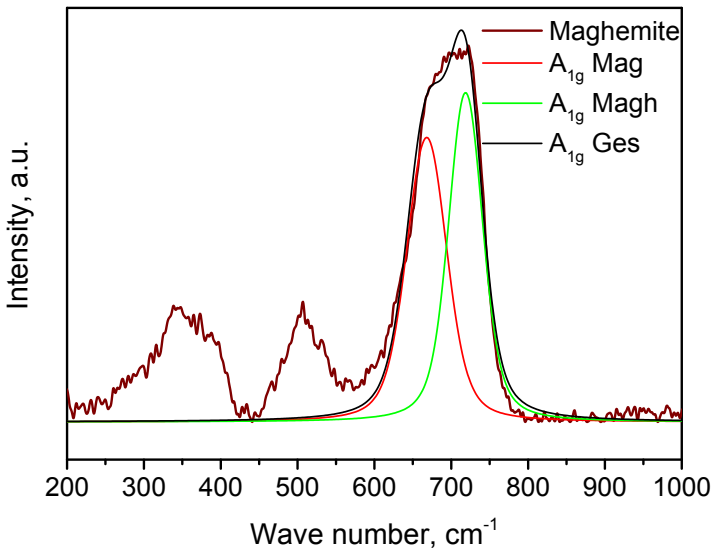


**Figure S19:** Raman spectrum of maghemite synthesised according to a method of Cornell and Schwertmann recorded with 488 nm at 0.4 mW.

**Table S20:** Phonon modes ($A_{1g}$ and $T_{2g}$ modes) of the synthesised and oxidised nanoparticles as measured with Raman spectroscopy.

| Time (min) | $A_{1g}$ (Mag) | $A_{1g}$ (Magh) | $T_{2g}/E_g$ | $T_{2g}$ |
|---|---|---|---|---|
| 0 | 665 | 720 | 536 | 318 |
| Air | | | | |
| 15 | 664.5 | 712.0 | 534 | 317 |
| 45 | 667.3 | 712.0 | 528 | 308 |
| 120 | 663.5 | 715.2 | 533 | 323 |
| 240 | 662.2 | 715.1 | 519 | 323 |
| 420 | 669.0 | 713.7 | 513 | 354 |
| 1440 | 664.0 | 711.3 | 510 | 355 |
| HNO3 | | | | |
| 1 | 669.8 | 718.5 | 532 | 330 |
| 15 | 667.5 | 712.0 | 519 | 333 |
| 45 | 666.8 | 712.0 | 519 | 352 |
| 120 | 667.7 | 715.0 | 509 | 352 |
| 240 | 664.0 | 713.3 | 505 | 360 |
| 1080 | 663.0 | 713.2 | 511 | 360 |
| 1440 | 662.0 | 719.0 | 505 | 359 |

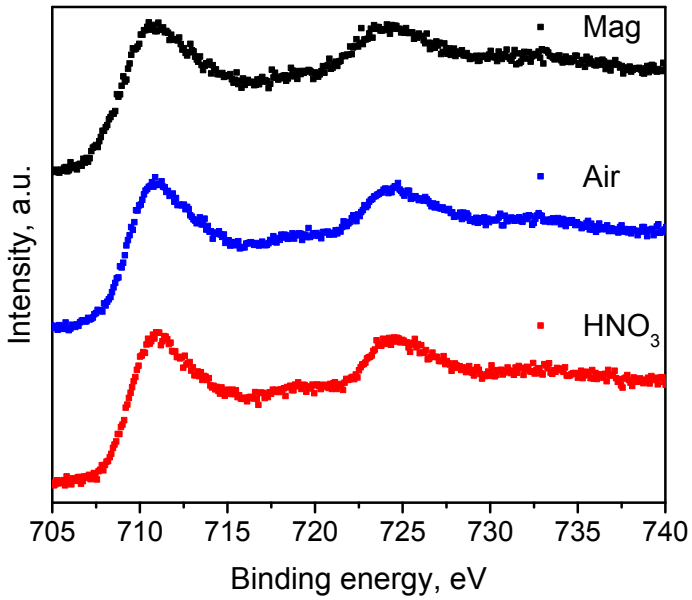


**Figure S21:** XP spectrum of magnetite and oxidised particles in the Fe 2p region.

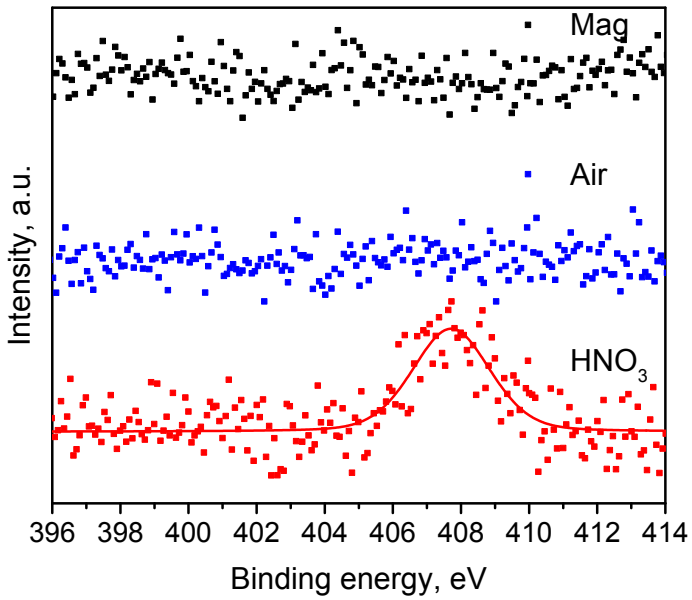


**Figure S22:** XP spectrum of magnetite and oxidised particles in the N 1s region.

**Calculation of magnetite content in nanoparticle samples**

Mössbauer spectroscopy:

$$Magnetite\ (\%) = 100\left(A\left(Fe^{2+} + Fe^{3+}\right) - 3 \cdot \left(\frac{A\left(Fe^{2+} + Fe^{3+}\right)}{3} - A\left(Fe^{2+}\right)\right)\right)$$

Raman spectroscopy:

$$Magnetite\ (\%) = 100 \cdot \left(1 - \frac{A(710\ nm)}{A(660\ nm)}\right)$$

X-ray diffraction:

$$Magnetite\ (\%) = 100 \cdot \left(\frac{A(Magn440)}{A(Magn440) + A(Magh440)}\right)$$

**Zeta potential**

Zeta potentials were measured with a Delsa Nano C Particle Analyser from Beckman Coulter, US. Samples were diluted to a concentration of 0.5 g $L^{-1}$. Zeta potential was recorded from pH 4 to pH 10 with HCl and NaOH as titrands.

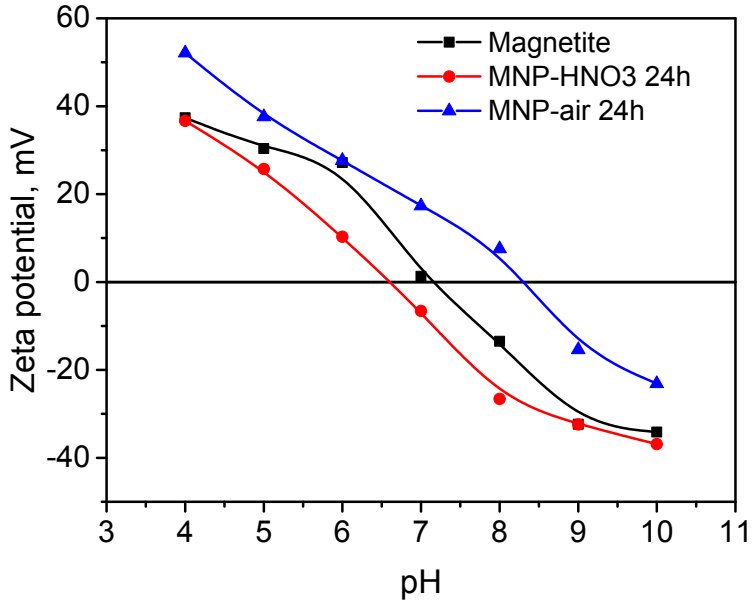


**Figure S23:** Zeta potential of synthesised magnetite and the particles oxidized under mild and harsh conditions. HCl and NaOH were used as titrands and the ionic strength was below 10 mM NaCl for the whole titration.

**Catalytic activity**

The catalytic activity was tested with the degradation of the dye rhodamine 6G purchased from Sigma-Aldrich. Therefore, a vessel of 50 mL containing particles (1 g $L^{-1}$) adjusted to a pH of 2 with sulfuric acid was incubated with 50 µmol $L^{-1}$ and 50 µL 30% $H_2O_2$ (Sigma-Aldrich) were added. The suspension was irradiated with UV light with an intensity of approximately 8 W. Aliquots were drawn after 5, 10, 15 and 30 minutes and filtered before being measured with an Infinite M200 Microplate Reader (Tecan Deutschland, Germany).at 530 nm. A similar experiment was conducted without $H_2O_2$ to calculate the adsorbed amount of rhodamine 6G.

Fenton reaction:

$$Fe^{2+} + H_2O_2 \rightarrow Fe^{3+} + HO\cdot + OH^-$$

$$Fe^{3+} + H_2O_2 \rightarrow Fe^{3+} + HOO\cdot + H^+$$

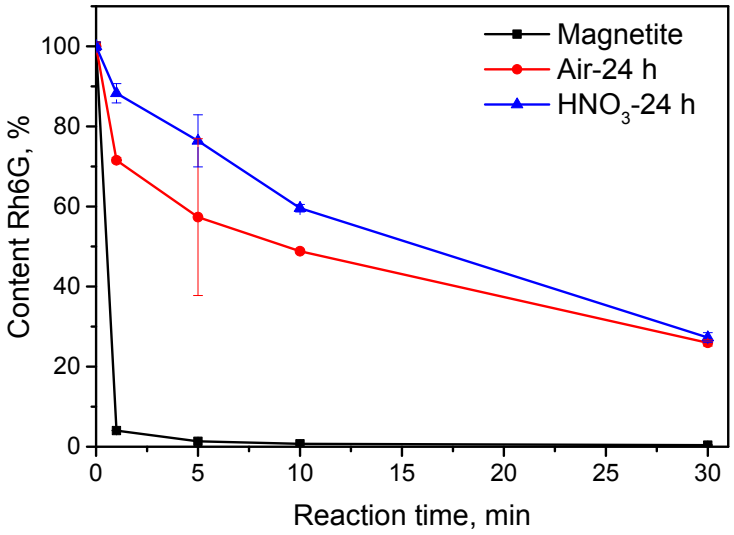


**Figure S24:** Catalytic degradation of the dye Rhodamine 6G for magnetite and fully oxidised particles.

## Toxicity tests

*Escherichia coli* HMS174(DE3) pET28a was used in this study. A pre-culture was performed in LB medium at pH 7.4 with kanamycine (50 µg $mL^{-1}$) over night at 37°C. The OD600 of the culture was adjusted to a value of 1 before the suspension was diluted to a concentration of approximately 8x103 bacteria $mL^{-1}$. 100 mL bacteria suspensions were incubated with different particle concentrations (10000, 1000, 100, 10 mg $L^{-1}$) and plated on LB-agar plates with kanamycine and therefore diluted by a factor of 10. The agar plates were incubated for 16 h at 37°C and the colonies were counted.

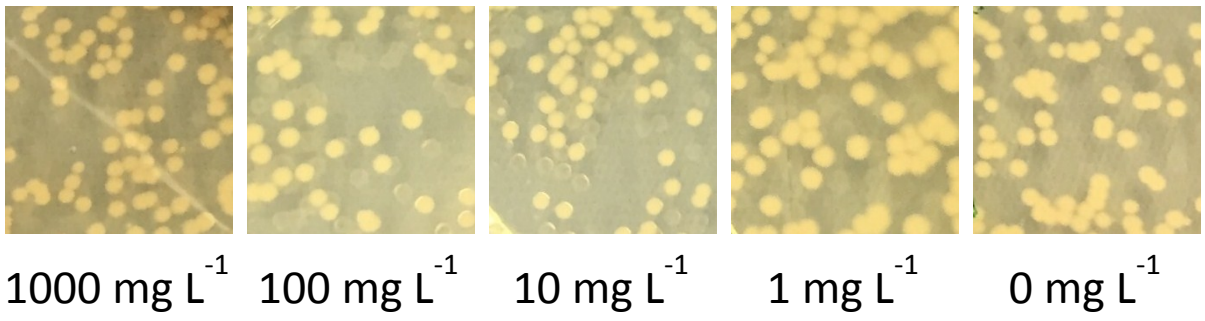


**Figure S25:** Bacteria colonies grown on LB-agar plates while being incubated with different concentrations of magnetite nanoparticles.

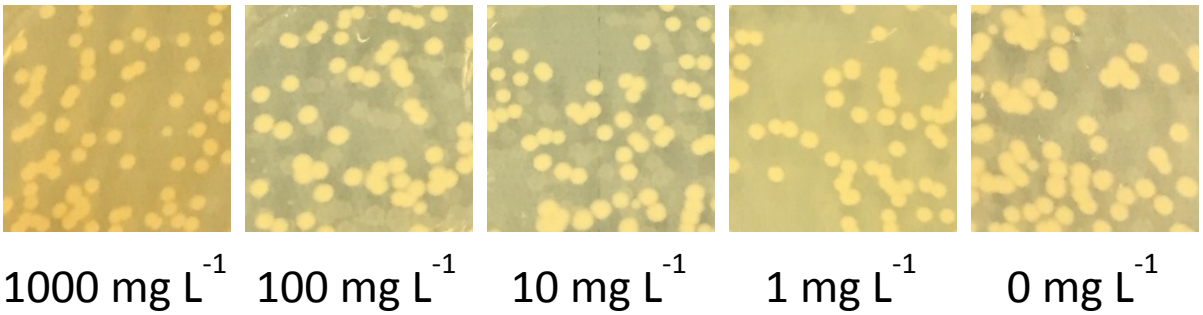


**Figure S26:** Bacteria colonies grown on LB-agar plates while being incubated with different concentrations of oxidised particles for 24 h at 60°C in air atmosphere.

**Table S27:** Number counts of bacteria colonies grown on LB-agar plates while being incubated with different concentrations of oxidised particles for 24 h at 60°C in air atmosphere.

| | Magnetite | Air-24h |
|---|---|---|
| 0 mg/L | 195 | 195 |
| 1 mg/L | 244 | 159 |
| 10 mg/L | 214 | 140 |
| 100 mg/L | 160 | 145 |
| 1000 mg/L | 215 | 165 |